Tetrahedron Letters 51 (2010) 2951–2955

Contents lists available at ScienceDirect

Tetrahedron Letters

journal homepage: www.elsevier.com/locate/tetlet

Reaction of N^3-phenylbenzamidrazone with *cis*-1,2-cyclohexanedicarboxylic anhydride

Marta Ziegler-Borowska [a], Marzena Ucherek [b], Jolanta Kutkowska [c], Liliana Mazur [c], Bożena Modzelewska-Banachiewicz [b], Dariusz Kędziera [a], Anna Kaczmarek-Kędziera [a,*]

[a] Faculty of Chemistry, Nicolaus Copernicus University, Gagarina 7, 87-100 Toruń, Poland
[b] Collegium Medicum, Nicolaus Copernicus University, 85-094 Bydgoszcz, Poland
[c] Department of Chemistry, Maria Curie-Skłodowska University, 20-031 Lublin, Poland

ARTICLE INFO

Article history:
Received 18 December 2009
Revised 26 March 2010
Accepted 29 March 2010
Available online 1 April 2010

ABSTRACT

An analysis of the products of the reaction of N^3-phenylbenzamidrazone with *cis*-1,2-cyclohexanedicarboxylic anhydride at various temperatures is presented. The identification of the reaction products is carried on with the support of computational techniques. The most stable conformers of the isoindole and triazole derivatives are found within the DFT approach. The theoretical calculations reveal the possible structure of a triazole derivative not available experimentally because of the presence of two diastereoisomers of equal energy.

Amidrazones have been shown to act as important precursors or intermediates in the synthesis of various chemical compounds widely applied in industry.[1] Moreover, the amidrazone moiety (the NCNN group) is an essential part of numerous molecules demonstrating high biological activity. Examples of bioactive amidrazone derivatives include vardenafil (Levitra) and lamotrigine (Lamictal). Vardenafil inhibits phosphodiesterase type 5 (PDE5) and is used in the treatment of erectile disfunction. Lamotrigine is a well-known anticonvulsant agent. Furthermore, open chain or cyclic derivatives of amidrazones and their metal complexes are known to exhibit antithrombotic,[3,2] antiinflammatory, antifungal, antimycobacterial,[4–6] antimalarial,[7] antihypertensive,[8] anticancer,[7,10,9,11] cytotoxic[12] and insulin-mimetic[13] activity. In organic synthesis, amidrazone derivatives have been found to be effective building blocks for nitrogen heterocyclic ring systems. By introducing an electron-withdrawing group on the amidrazone moiety the relative reactivity of the three *N*-nucleophiles in the molecule can be modified. This has an important consequence in synthetic chemistry, leading to regiocontrolled reactions.[14,15]

For the above-mentioned reasons the chemistry of amidrazones has been widely studied. However, only recently has the synthetic significance of N^3-substituted amidrazones been noticed.[16] The reaction of N^3-substituted amidrazones with maleic anhydride always leads to 3-(3,4-diaryl-1,2,4-triazol-5-yl)propenoic acid derivatives, irrespective of the amidrazone substituents (Scheme 1). Some of the synthesized 1,2,4-triazoles show anticonvulsive and antinociceptive activity and have been reported as effective agents against a number of bacterial species.[16]

Despite the interesting chemistry and numerous applications of isoindole or 1,2,4-triazole derivatives, hardly any data on this class of compounds are present in the literature.[20,18,21,17,19] Therefore, the aim of the present contribution is the analysis of the products of the reaction of N^3-phenylbenzamidrazone **1** with *cis*-1,2-cyclohexanedicarboxylic anhydride **2** at various temperatures. The synthetic and analytical part of the project are supported by computational investigations.

N^3-Phenylbenzamidrazone **1** was synthesized by the method described earlier in the literature.[22,23] *cis*-1,2-Cyclohexanedicarboxylic anhydride **2** is available commercially.

The substrates were dissolved in anhydrous toluene prior to mixing them together in the molar ratio 1:1. Whereas the cyclocondensation reaction of compound **1** with *cis*-1,2-cyclohexanedicarboxylic anhydride in boiling toluene (Scheme 2) gave the

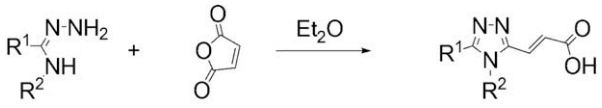

R^1 = Ph, 2-Py, 4-Py

R^2 = Ph, 4-MeC_6H_4, 4-$O_2NC_6H_4$, 4-Py.

Scheme 1.

* Corresponding author. Fax: +48 56 654 24 77.
E-mail address: teoadk@chem.umk.pl (A. Kaczmarek-Kędziera).

0040-4039/$ - see front matter © 2010 Elsevier Ltd. All rights reserved.
doi:10.1016/j.tetlet.2010.03.116

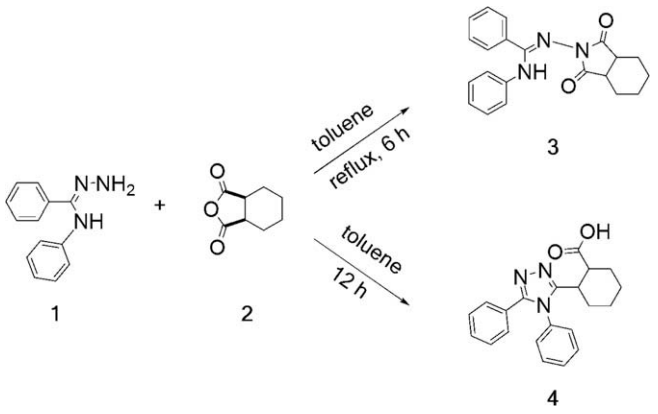

Scheme 2.

cyclic imide **3** in 78% yield, reaction in anhydrous toluene at room temperature led to the formation of the heterocyclic five-membered ring system **4** (Scheme 2) in 75% yield.

In contrast to these findings, our recent work has shown that from the reactions of N^3-(2-pyridyl)-2-picolinamidrazone and N^3-4-nitrophenyl-2-picolinamidrazone with *cis*-1,2-cyclohexanedicarboxylic anhydride, only linear derivatives, exhibiting antiproliferative activity, were obtained: *N*-carbonyl-[(2-carboxycyclohexane-1-yl)-N^3-pyridin-2-yl]-2-picolinamidrazone and N^1-carbonyl-[(2-carboxy-cyclohexane-1-yl)-N^3-4-nitrophenyl]-2-picolinamidrazone (Scheme 3). All the above-mentioned reactions were performed in anhydrous diethyl ether at room temperature. These results suggest that not only the reaction conditions but also the structure of the substrates (amidrazone and anhydride) may determine the direction of the investigated reaction.

The size of the investigated system significantly reduces the number of computational methods available and eliminates high-level ab initio ('post-Hartree-Fock') approximation. However, since the main attention of the current project is focused on the structures of the reagents, considerations within the density functional theory are expected to provide at least qualitatively correct results. Therefore, the structure of the stationary points on the potential energy surface has been determined within the B3LYP/6-31+G(d) approach. The character of the stationary points was verified by harmonic vibrational analysis. Hence, all the reactions in vitro are performed in organic solvents, the in silico simulations include solvent effects via the continuum solvent model (IEF-PCM). All calculations were carried out using GAUSSIAN03. [24]

A thorough study of the potential energy surface (PES) of **3** was initially performed in the gas phase. Local minima on the PES were located within the B3LYP/6-31+G(d) approach for compound **3** via rotation along the single C13–N15 and N8–N12 bonds in the amidrazone moiety and included the *exo*–*endo* isomers in the anhydride system. Various conformations of compound **3** were obtained this way, however, four seemed to be significantly more stable energetically. The energy differences among these four isomers were small and all were found in the 1 kcal/mol energy gap (see Table 1). The lowest-energy form, **3b**, is presented in Figure 1. Such a small energy difference suggests that the energetic order is very sensitive to the approximation choice. Hence, the larger basis set 6-311++G(d,p) was applied to confirm the data. However, it did not change the stability order of the four lowest-energy forms of compound **3**. Moreover, the rotation along the single C13–N15 bond is low-barrier: the rotation requires 4–8 kcal/mol depending on the conformation. Therefore, the isoindolic amidrazone derivatives are flexible and can undergo rotation relatively easily. The inclusion of solvent effects in the calculations via the IEF-PCM model leads to narrowing of the energetic differences between the various conformers. Additionally, a change of the energetic order is observed in the case of the four lowest-energy forms. The calculated energy difference between the two forms *endo* and *exo* (**3a** and **3a′**) is virtually zero. Both are additionally stabilized by an intramolecular hydrogen bond like interaction. Applying the larger, 6-311++G(d,p), basis set clearly indicates the lowest-energy conformer corresponding to the crystallographic structure. Within this approximation the **3a** form becomes 2.3 kcal/mol more stable than that of **3a′**. The geometrical parameters (bond lengths, valence angles and dihedral angles) from the crystallographic data (Figure 2) and computations are available in the Supplementary data.

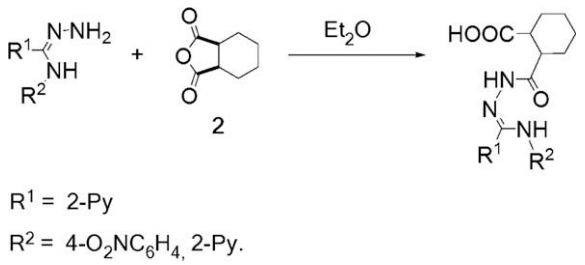

Scheme 3.

Table 1
Relative energies of the conformers of the low-energy isoindole derivative **3**

Conformation	Relative energy		
	Gas phase		PCM (benzene)
	6-31+G(d)	6-311++G(d,p)	6-31+G(d)
3a	1.01	0.70	0.05
3a′	0.75	0.45	0.00
3b	0.00	0.00	0.52
3b′	0.27	0.22	0.70

All values in kcal/mol. Computational data obtained within the B3LYP approximation.

Numerous minima on the PES in the gas phase were localized computationally for compound **4**. There are two stereogenic carbons in the cyclohexyl moiety: C6 and C11, therefore, the molecule can exist in various stereoisomeric forms. Figure 3 presents the two lowest-energy diastereoisomers of **4** (**4a** and **4b**). The lowest-energy rotamer tends to the maximal separation of the substituents and therefore, minimization of the intramolecular interactions between the terminal groups. The existence of isoenergetic equivalent forms results in the presence of various forms in the reaction mixture and makes simple crystallization impossible.

Two other forms of **4** differing only by slight rotation of the phenyl rings can be found at 0.88 kcal/mol on the energy scale. Next, at 1.62 kcal/mol higher than the lowest-energy conformers, the two isoenergetic isomers appear different from those depicted in Figure 3 by rotation of the hydroxy group in the direction of the triazole ring N5 nitrogen, and they form weak intramolecular hydrogen bond like interactions. However, the energy of the H-bonded systems is relatively high with respect to the lowest-energy rotamers. Moreover, since the low-energy forms are separated by the relatively low rotation barrier, interconversion of the corresponding rotamers is possible under the reaction conditions.

The forms presented above correspond to the trans isomer of the substituted cyclohexyl moiety. A similar situation occurs with the *cis*-configured isomer, when the carboxyl group is placed in the axial position. The lowest-energy *cis* diastereoisomers lie 3.46 kcal/mol above the **4a** and **4b** forms.

The steric strain in the cyclohexyl group disfavours the boat conformation considerably. The boat isomers appear higher in

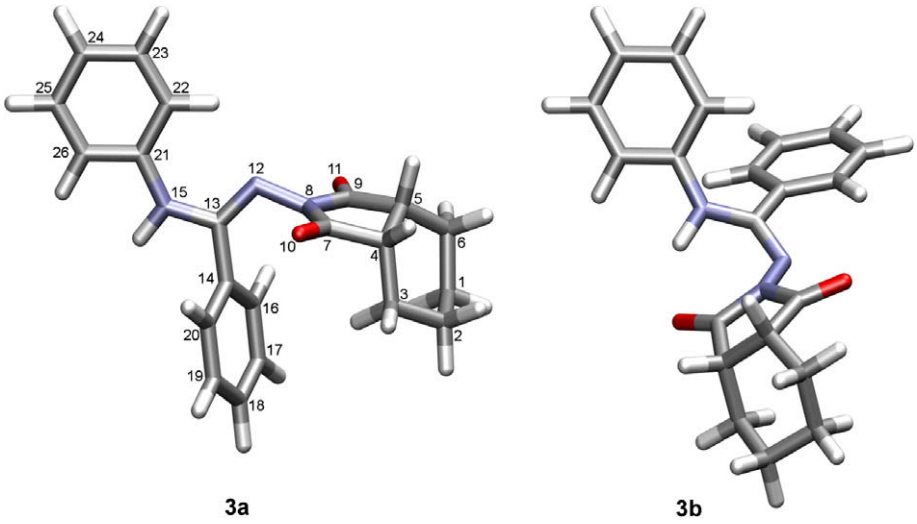

Fig. 1. Two low-energy conformers of isoindole derivative **3**. Nitrogen atoms are depicted in blue, oxygen atoms in red, carbon atoms in grey and hydrogens in white.

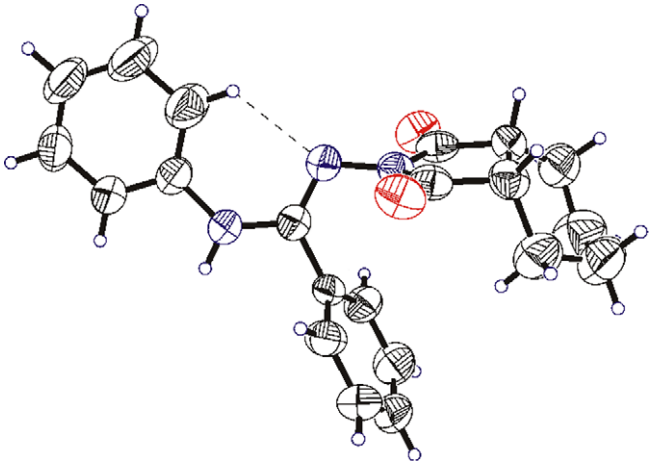

Fig. 2. The crystal structure of **3** (CCDC 756299). The displacement ellipsoids are drawn at the 50% probability level. Dashed line indicates a hydrogen bond. Crystal atom numbers are available in the Supplementary data.

energy by more than 6 kcal/mol compared with the lowest-energy forms.

The IR spectrum measured experimentally for isoindole derivative **3** has been compared with unscaled computational harmonic vibrational frequencies to simplify its interpretation. The corresponding data are presented in Table 2. The presence of the non-polar solvent within the IEF-PCM approach does not affect the computed values of the harmonic frequencies for **3** significantly. Although the theoretically predicted spectra, both in the gas phase and in solvent, are significantly blue-shifted with respect to the experimental, the calculations reveal the same structures for the spectra and help to identify the origin of the individual signals precisely.

^{1}H NMR chemical shifts calculated theoretically are juxtaposed with the experimental results in Table 3. It is known that reproduction of the NMR shifts for labile protons can be problematic.[25] Also in the present study, the calculations in the gas phase or in the solvent described by the continuum IEF-PCM model are not sufficient for our purpose: the gas phase calculations recover 78% of the chemical shift value for **3** and only 46.7% for **4**, while the PCM calculations give 82.3% of the experimental result for **3** and only 60.8% for **4**. This is caused by the potential hydrogen bonds that can form between the analyzed system and the solvent (DMSO) molecules and are not described by the continuum solvation models. However, explicit inclusion of the first solvation shell can improve the obtained data significantly. [26] Since the size of the investigated species and the solvent (DMSO) molecules prohibit use of the full first solvation shell for **3** and **4**, in the present study, just one DMSO molecule was added to the investigated species in the gas phase in such a way as to make H-bonding with the labile protons possible (for the analyzed structures, see Figure 4). It can be seen from Table 3 that such a simple manipulation shifts the corresponding signal in the gas phase from 7.575 to 8.548 ppm for **3** and from 5.563 to 10.912 ppm for **4**. Therefore, the inclusion of the continuum sol-

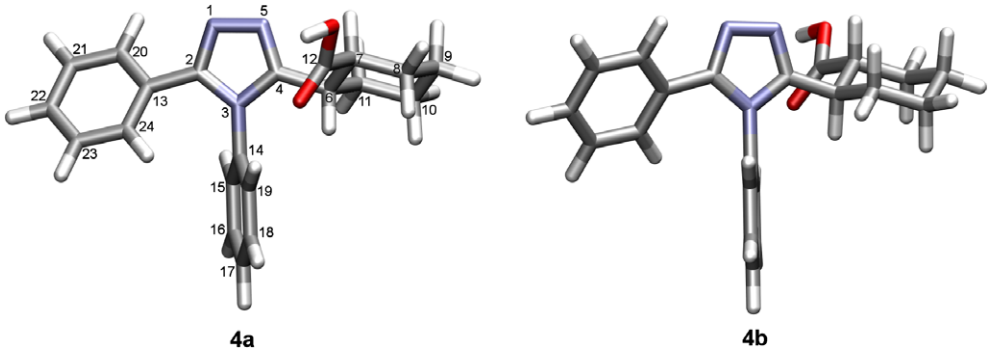

Fig. 3. Lowest-energy diastereoisomers of triazoles **4**, **4a** and **4b**. Nitrogen atoms are depicted in blue, oxygen atoms in red, carbon atoms in grey and hydrogens in white.

Table 2
IR spectrum of isoindole derivative **3** and triazole **4** determined experimentally and computationally

Vibration	3			4	
	Exp.	Calcd (gas)	Calcd (benzene)	Exp.	Calcd (gas)
N–H stretch	3312	3614	3552		
C=N stretch				1598	1540
O–H stretch				3405	3681
C–H stretch (arom)	3132	3270, 3212, 3209 3207, 3200, 3195 3193, 3186, 3184 3163	3266, 3197, 3191 3190, 3182, 3177 3174, 3168, 3166 3150	3182	3181, 3187, 3192 3196, 3204, 3205 3212, 3225, 3228 3228
C–H stretch (aliph)	2920	3098, 3091, 3081 3074, 3070, 3038 3037, 3028, 3018 3010	3091, 3087, 3071 3069, 3068, 3037 3035, 3025, 3016 2995	2920	3018, 3024, 3029 3040, 3061, 3068 3072, 3078, 3085 3095
C=O	1630	1831, 1766	1819, 1747	1630	1800
Aromatic bending (asym)	1598	1654, 1652, 1641 1626	1651, 1649, 1634 1624	1598	1630, 1638, 1651 1656
Aromatic bending (sym)	1466	1538, 1536	1535, 1533	1466	1480, 1492, 1541 1559

Vibrational frequencies in cm^{-1}. Computational values are unscaled.

Table 3
^1H NMR computational and experimental chemical shifts with respect to TMS [ppm]

	3				4			
	Exp. (DMSO)	Calcd (gas)	Calcd (PCM)	Calcd (DMSO)	Exp. (DMSO)	Calcd (gas)	Calcd (PCM)	Calcd (DMSO)
Aliphatic CH_2	0.814–1.415	1.299–2.607	1.396–2.405	−0.192–2.464	1. 328–2.497	1.247–2.173	1.334–2.180	1.110–2.305
Aliphatic CH	2.763	2.709–2.710	3.221–3.261	2.334–2.563	2.565–3.212	2.361–3.538	2.407–3.530	2.717–3.466
Aromatic CH	7.044–7.804	6.074–8.465	6.205–8.399	6.954–8.811	7.278–7.580	6.431–8.328	6.644–8.285	6.287–8.618
NH (**3**)/OH (**4**)	9.644	7.575	7.952	8.548	12.038	5.563	7.329	10.912

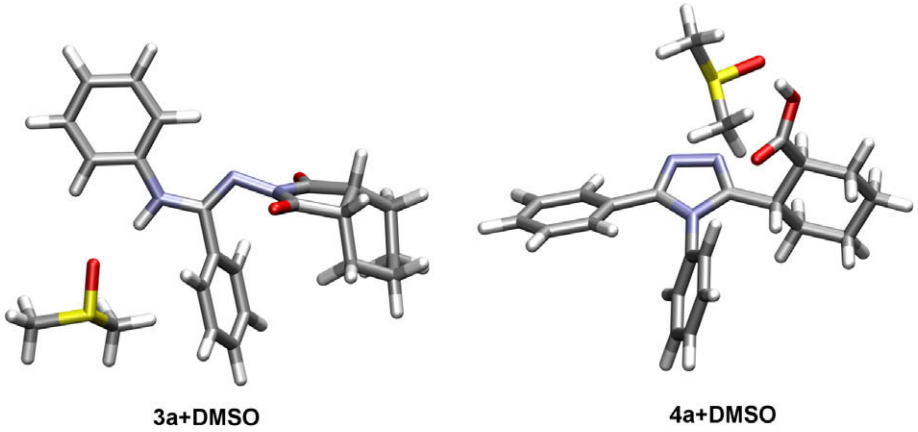

Fig. 4. The lowest-energy conformers of **3** and **4** with one DMSO molecule. Nitrogen atoms are depicted in blue, oxygen atoms in red, carbon atoms in grey, sulfur atoms in yellow and hydrogens in white.

vent medium improves the data by about 5% for **3** and 15% for **4**, however, the addition of just one solvent molecule gives an improvement of 10% with respect to the gas phase calculations for **3** and up to 45% for **4**. While the improvement for **3** is relatively small, because the original error is not that large, the correction for **4** is huge and gives calculated results close to the experimental with satisfactory accuracy and relatively small computational cost. Further improvement is not crucial for the purpose of qualitative comparison of the computational and experimental data to interpret the experimental spectrum. This can be achieved by increasing the basis set size and flexibility, however, this results in a significant growth in computational time.

The standard reference strains (American Type Culture Collection) and bacterial strains isolated from human clinical materials were used to study the antibacterial activity. The following strains

Table 4
Minimum inhibitory concentrations of compounds **3** and **4** (μg/mL)

Bacteria	MIC	
	3	**4**
Escherichia coli ATCC 25922	500	500
Pseudomonas aeruginosa ATCC 27853	500	500
Yersinia enterocolitica O3	250	100
Enterococcus faecalis ATCC 29212	100	250
Sarcina lutea	250	250
Staphylococcus aureus ATCC 25923	250	500
Nocardia spp.	500	250
Rhodococcus equi	500	100
Mycobacterium smegmatis	500	250
Candida albicans	250	100

were tested: Gram-negative bacteria *Escherichia coli* ATCC 25922, *Pseudomonas aeruginosa* ATCC 27853, *Yersinia enterocolitica* O3; Gram-positive *Enterococcus faecalis* ATCC 29212, *Sarcina lutea*, *Staphylococcus aureus* ATCC 25923; *Nocardia* spp., *Rhodococcus equi*, *Mycobacterium smegmatis* and the pathogenic fungus *Candida albicans*. The results are presented in Table 4.

The sensitivities to the derivatives **3** and **4** were of similar orders of magnitude (MIC 100–250 μg/mL) for the following strains: Gram-positive bacteria *S. lutea* and *E. faecalis* ATCC 29212; Gram-negative *Y. enterocolitica* O3 and the fungus *C. albicans*. Moreover, **3** was also active against *S. aureus* ATCC 25923, while **4** exhibited a relatively high antibacterial potency against *R. equi*, *M. smegmatis* and *Nocardia* (MIC 100–250 μg/mL). Both tested compounds did not inhibit the growth of the bacterial strains used as drug resistant markers, *E. coli* ATCC 25922 and *P. aeruginosa* ATCC 27853. Hence, one should note that the presented data predict good selectivity for **3** and significant activity only with respect to *E. faecalis*.

In the present contribution the synthesis of two novel triazole and isoindole derivatives is described. The current results suggest that the products of the reaction of the amidrazone with the acid anhydride depends on the temperature. The reaction performed at room temperature leads to the triazole **4**, while at increased temperatures the isoindole derivative **3** is obtained. Further investigation of the factors influencing the direction of the reaction is necessary. The analyzed compounds exhibit biological activity and **3** can selectively inhibit the growth of *E. faecalis*. This result alludes to selective drug design in pharmacology. The experimental work was supported by the theoretical calculations. A detailed study of the potential energy surface of **3** leads to results closely reproducing the crystallographic data, therefore, the established methodology was further applied to predict the structure of the triazole derivative **4**, for which crystals are not available. Moreover, the NMR shift calculations offer a simple method to predict the ^{1}H NMR shifts for the labile protons with relatively good accuracy with not too high computational cost.

Acknowledgements

The authors are indebted to Dr. Andrzej Wolan for technical support and fruitful discussions. Wrocław Supercomputing and Networking Center, AGH Cyfronet Kraków and Poznań Networking and Supercomputing Center are gratefully acknowledged for the generous allotment of computational resources.

Supplementary data

Geometrical parameters for the crystal of the isoindole derivative **3** and lowest-energy conformer computational geometrical data are available. Atom numbering in the crystal. Supplementary data associated with this article can be found, in the online version, at doi:10.1016/j.tetlet.2010.03.116.

References and notes

1. Neilson, D. G.; Heatlie, J. W. M.; Newlands, L. R. *Chem. Rev.* **1970**, *70*, 151.
2. Lee, K.; Hwang, S. Y.; Hong, S.; Hong, C. Y.; Lee, C.-S.; Shin, Y.; Kim, S.; Yun, S.; Yoo, Y. J.; Kang, M.; Oh, Y. S. *Bioorg. Med. Chem.* **1998**, *6*, 869.
3. Song, Y.; Clizbe, L.; Bhakta, C.; Teng, W.; Wong, P.; Huang, B.; Tran, K.; Sinha, U.; Park, G.; Reed, A.; Scarborough, R. M.; Zhu, B.-Y. *Bioorg. Med. Chem. Lett.* **2003**, *13*, 297.
4. Coleman, M. D.; Rathbone, D. L.; Endersby, C. R.; Hovey, M. C.; Tims, K. J.; Lambert, P. A.; Bilington, D. C. *Environ. Toxicol. Pharmacol.* **2000**, *8*, 167.
5. Mamolo, M. G.; Falagiani, V.; Vio, L.; Banfi, E. *Farmaco* **1999**, *54*, 761.
6. Ranft, D.; Lehwark-Yvetot, G.; Schaper, K.-J.; Buge, A. *Arch. Pharm. Pharm. Med. Chem.* **1997**, *330*, 169.
7. Gokhale, N. H.; Padhye, S. B.; Bilington, D. C.; Rathbone, D. L.; Croft, S. L.; Kendrick, H. D.; Anson, C. E.; Powell, A. K. *Inorg. Chim. Acta* **2003**, *349*, 23.
8. Mamolo, M. G.; Pellizer, G. *Arch. Pharm.* **1988**, *321*, 713.
9. Gokhale, N. H.; Padhye, S. B.; Rathbone, D. L.; Bilington, D. C.; Rathbone, D. L.; Lowe, P.; Schwalbe, C.; Newton, C. *Inorg. Chem. Commun.* **2001**, *4*, 26.
10. Pelova, R.; Spassowska, N.; Manieva, L.; Taxirov, S. *Pharmazie* **1987**, *42*, 251.
11. Radwan, M. A. A.; El-Sherbiny, M. *Bioorg. Med. Chem.* **2007**, *15*, 2106.
12. Ponticelli, G. *Trans. Met. Chem.* **2006**, *31*, 703.
13. Cocco, M. T.; Onnis, V.; Ponticelli, G.; Meier, B.; Rehder, D.; Garribba, E.; Micera, G. *J. Inorg. Chem.* **2007**, *101*, 19.
14. Adam, F. M.; Burton, A. J.; Cardwell, K. S.; Cox, R. A.; Henson, R. A.; Mills, K.; Prodger, J. C.; Schilling, M. B.; Tape, D. T. *Tetrahedron Lett.* **2003**, *44*, 5657.
15. Adamo, M. F. A.; Baldwin, J. E.; Adlington, R. M. *J. Org. Chem.* **2005**, *70*, 3307.
16. Modzelewska-Banachiewicz, B.; Banachiewicz, J.; Chodkowska, A.; Jagiełło-Wójtowska, E.; Mazur, L. *Eur. J. Med. Chem.* **2004**, *39*, 873.
17. Bonnet, R.; North, S. A.. In *Advances in Heterocyclic Chemistry*; Academic Press: New York, 1981; Vol. 29.
18. Ferenc, C.; Stajer, G. *Curr. Org. Chem.* **2005**, *9*, 1261.
19. Garrat, P. J.. In *Comprehensive Heterocyclic Chemistry II*; Pergamon Press: New York, 1996; Vol. 4.
20. Marinicheva, G. E.; Gubina, T. I. *Chem. Heterocycl. Compd.* **2004**, *40*, 12.
21. White, J. D.; Mann, M. E.. In *Advances in Heterocyclic Chemistry*; Academic Press: New York, 1969; Vol. 10.
22. Spasow, A.; Golovinskii, E.; Demirov, G. *Chem. Ber.* **1965**, *98*, 932.
23. Wallach, O.; Liebigs, J. *Ann. Chem.* **1890**, *259*, 301.
24. Frisch, M. J.; Trucks, G. W.; Schlegel, H. B.; Scuseria, G. E.; Robb, M. A.; Cheeseman, J. R.; Montgomery; Jr.; A., J.; Vreven, T.; Kudin, K. N.; Burant, J. C.; Millam, J. M.; Iyengar, S. S.; Tomasi, J.; Barone, V.; Mennucci, B.; Cossi, M.; Scalmani, G.; Rega, N.; Petersson, G. A.; Nakatsuji, H.; Hada, M.; Ehara, M.; Toyota, K.; Fukuda, R.; Hasegawa, J.; Ishida, M.; Nakajima, T.; Honda, Y.; Kitao, O.; Nakai, H.; Klene, M.; Li, X.; Knox, J. E.; Hratchian, H. P.; Cross, J. B.; Bakken, V.; Adamo, C.; Jaramillo, J.; Gomperts, R.; Stratmann, R. E.; Yazyev, O.; Austin, A. J.; Cammi, R.; Pomelli, C.; Ochterski, J. W.; Ayala, P. Y.; Morokuma, K.; Voth, G. A.; Salvador, P.; Dannenberg, J. J.; Zakrzewski, V. G.; Dapprich, S.; Daniels, A. D.; Strain, M. C.; Farkas, O.; Malick, D. K.; Rabuck, A. D.; Raghavachari, K.; Foresman, J. B.; Ortiz, J. V.; Cui, Q.; Baboul, A. G.; Clifford, S.; Cioslowski, J.; Stefanov, B. B.; Liu, G.; Liashenko, A.; Piskorz, P.; Komaromi, I.; Martin, R. L.; Fox, D. J.; Keith, T.; Al-Laham, M. A.; Peng, C. Y.; Nanayakkara, A.; Challacombe, M.; Gill, P. M. W.; Johnson, B.; Chen, W.; Wong, M. W.; Gonzalez, C.; Pople, J. A. GAUSSIAN *03*. Gaussian, Wallingford, CT, 2004.
25. Siwek, A.; Wujec, M.; Wawrzycka-Gorczyca, I.; Dobosz, M.; Paneth, P. *Heteroat. Chem.* **2008**, *19*, 337.
26. Dracinsky, M.; Bour, P. *J. Chem. Theory Comput.* **2010**, *6*, 288.